SCIENTIFIC AND APPLIED ASPECTS OF FERROMAGNETIC SHAPE MEMORY ALLOYS

V.A. Chernenko, S. Besseghini, F. Stortiero, T. Cavallin

The underlying mechanisms responsible for the giant magnetic or mechanical field-induced-strains in the Ni-Mn-Ga ferromagnetic shape memory alloys are briefly discussed. The fundamental aspect is illustrated by experimental data related to the lattice instability and composition dependence of magnetization alongside literature results. An implementation of Ni-Mn-Ga single crystal as a strain sensor is described.

KEYWORDS: shape memory alloys, intermetallics, properties, physical metallurgy

INTRODUCTION

It is desirable that the transducing materials show a combination of the large strains, high-force production and fast dynamic response during actuation event. Different actuator materials such as (ferro-)piezoelectric, magnetostrictive, shape-memory alloys (SMA's), rheological liquids etc. have been already elaborated and commercially incorporated into the modern technologies. The functionality of these materials is based on the physical mechanisms responsible for the electric, magnetic or thermal energy transformations into mechanical work, which produce the actuation. The reverse energy conversion is in use for sensing. The efficiency, power density and speed of the aforementioned types of energy conversion determine the advantages and drawbacks of these materials in the applications. As an example, a slow response due to thermal inertia is typical of the shape-memory materials, while their advantage lies in the more-than-one-order-of-magnitude larger reversible strains, compared with other materials in question.

The disadvantage of a slow-response of the ordinary SMA's can be overcome by using shape-memory materials which are also ferromagnetic. The latter materials emerged recently as a novel class of multifunctional materials denoted as ferromagnetic shape memory alloys (FSMA's) which combine the properties of ferromagnetism with those of a thermoelastic martensitic transformation [1-3]. In particular, FSMA's in their martensitic state allow for a stress- or magnetic-field-induced rearrangement of twin variants resulting in a giant magnetostrain, 5-10% [4,5]. Prototype of the FSMA's is Ni_2MnGa Heusler alloy with its off-stoichiometric derivatives [1-6]. Other FSMA systems [3], such as Fe-Pd [1], Fe_3Pt [1], Ni-Mn-(Al, Sn, Sb, In) [7,8], Co-Ni-(Al, Ga) [9,10], Ni-Fe-(Al,Ga) [11,12] are of an increasing interest as well.

Till present, the best-working room-temperature easy-axis-ferromagnetic martensites in Ni-Mn-Ga alloys have been the subject of the most intense fundamental and applied research. For these alloys, a bulk single-crystalline technology was developed, which led to commercially available prototypes of actuators [13]. There exists also a large interest in thin-film technology of FSMA's for microsystem applications [14].

The underlying physical mechanisms of the giant magnetic or mechanical field-induced-strains (MFIS) in FSMA's are briefly explained in this work. Some experimental results on the Ni-Mn-Ga alloys are shown to highlight the most important fundamental ideas. An application of Ni-Mn-Ga single crystal as a strain sensor is described.

V.A. Chernenko, S. Besseghini, F. Stortiero, T. Cavallin
CNR-IENI, Unità Staccata di Lecco, Italia

PHENOMENOLOGY OF GIANT FIELD-INDUCED STRAINS IN FSMA'S

A. Lattice instability

An inherent lattice instability toward thermoelastic martensitc transformation (MT) is a basic reason explaining why ferromagnetic Ni-Mn-Ga alloys display a giant MFIS [15,16]. This instability is mainly related to a uniform (110)[1,-1,0] shear often accompanied by shuffling in the same system. It belongs to a Zener-type instability typical of ß-alloys when a parent phase with bcc open lattice transforms during cooling into a lower-symmetry close-packed martensitic phase as a result of the invariant-plane Bain deformation. In order to accommodate stresses due to the large Bain strains, secondary invariant-lattice strains occur involving the same shear system so that a twinned microstructure is formed.

It is worth noting that the aforementioned shear in Ni-Mn-Ga intermetallics, as well as in other ß-alloys, is characterized by a low restoring force, that is to say, their shear modulus C′ is very small. Moreover, C′ has an abnormal descending temperature dependence during cooling in the cubic phase down to a minimum of about a few GPa near MT [17,18]. Fig. 1 illustrates typical temperature evolutions of the low-frequency elastic modulus for three single crystalline Ni–Mn–Ga specimens belonging to the different groups [6]. The anomalies accompanying the different phase transformations can be observed in this figure where the arrows indicate the characteristic temperatures. The lattice instability of the parent phase when approaching T_M or T_I, which is a manifestation of precursor events, is evidenced by an almost linear softening of the elastic modulus, not only in ferromagnetic state but also in paramagnetic one. According to Fig. 1, the total decrease of modulus in the cubic phase can be 30 - 40 %.

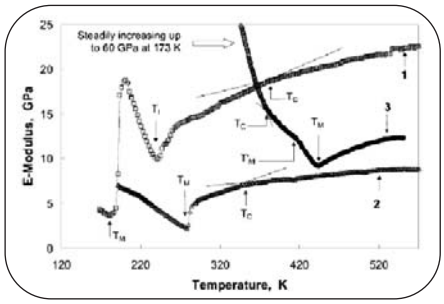

Fig. 1

Elastic modulus vs. temperature curves recorded during cooling for $Ni_{49.2}Mn_{26.6}Ga_{24.2}$, (curve 1); $Ni_{52.6}Mn_{23.5}Ga_{23.9}$ (curve 2) and $Ni_{51.2}Mn_{31.1}Ga_{17.7}$ (curve 3) [17]. The arrows indicate the temperatures corresponding to the different phase transitions: T_M holds for the martensitic transformation; T_I holds for the premartensitic transformation into the intermediate phase I; T'_M indicates the intermartensitic transformation and T_C is the Curie temperature.

Variazione del modulo elastico con la temperatura durante il raffreddamento per $Ni_{49.2}Mn_{26.6}Ga_{24.2}$, (curva 1); $Ni_{52.6}Mn_{23.5}Ga_{23.9}$ (curva 2) e $Ni_{51.2}Mn_{31.1}Ga_{17.7}$ (curva 3) [17]. Le frecce indicano le temperature di trasformazione di fase: T_M (trasformazione martensitica), T_I (trasformazione premartensitica da fase genitrice nella fase intermedia I), T'_M (trasformazione intermartensitica) e T_C (temperatura di Curie).

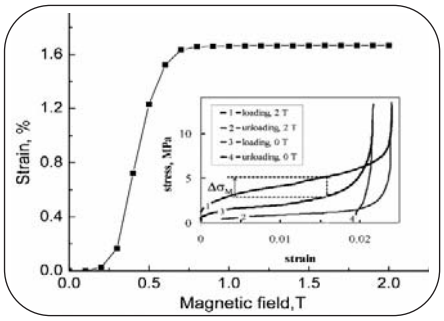

Fig. 2

Magnetic-field-induced strain measured at T=300 K along [100]$_C$ axis for a $Ni_{51.0}Mn_{27.9}Ga_{21.1}$ single-crystal with T_M=314 K and T_C=370 K. Inset: compressive stress-strain curves measured with orthogonal magnetic field for the same specimen at T=300K (see Ref. [21] for details).

Deformazione indotta da campo magnetico misurata a T=300 K lungo l'asse [100]$_C$ di un monocristallo di composizione $Ni_{51.0}Mn_{27.9}Ga_{21.1}$ con T_M=314 K e T_C=370 K. Nel dettaglio: curve stress-strain di compressione misurate sullo stesso campione con campo magnetico ortogonale a T=300K (per dettagli vedere rif. [21]).

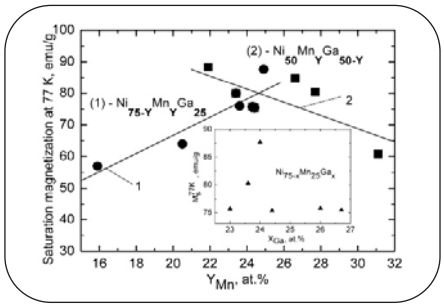

Fig. 3

Saturation magnetization measured at H=1 T and T=77 K as a function of composition for Ni-Mn-Ga alloys at a constant content of the third element. The straight lines are guides for the eye.

Magnetizzazione di saturazione misurata con H=1 T e a T=77 K in funzione della composizione per leghe Ni-Mn-Ga con contenuto in Ga costante. Le rette sono state tracciate come guida per l'osservazione.

One of the consequences of a small modulus, especially in the temperature range of structural transformations, is a considerably enhanced ordinary magnetostriction. For instance, at the parent-to-intermediate phase transition in Ni_2MnGa, it is about 600 ppm [19]. As far as the MT in this compound is concerned, the aforementioned value is about 10 times larger [19], which implies a predominant contribution of the reversible motion of twinning dislocation [20-22]. Alongside an abnormally reduced elastic modulus, Ni-Mn-Ga alloys in single-crystalline form are characterised by extremely mobile twin boundaries accounting for very low yield stresses, $\sigma_y \sim 1$ MPa, in the martensitic state [21,22]. Such a twinning stress appears smaller than the equivalent mechanical stress (magnetostress) produced by a magnetic field which explains the giant magnetostrain effect.

B. Concept of magnetostress

The martensitic transformation in Ni-Mn-Ga alloys is accompanied by a cubic-to-tetragonal unit cell distortion with a contracted c-axis and expanded a-axes. The magneto-elastic coupling described by a negative magnetostriction constant is responsible for the appearance of an easy-magnetization direction along the short c-axis accompanied by the large uniaxial magnetic anisotropy. It is also responsible for the emergence of magnetostress. The phenomenological and microscopic models suggesting the equivalence of magnetic field and stress in a ferromagnetic martensite are presented in Refs.[20,23].

In the phenomenological magnetoelastic model of ferromagnetic martensite [22-24], this equivalence stems from energy density terms like $\sim M^2\varepsilon$ describing magnetoelastic interaction, where M and ε are the appropriate components of magnetization vector and strain tensor, respectively. Basically, the above terms arise because spin exchange and spin-orbit interactions between the electrons depend on the atom coordinates. The core structure of the Helmholtz free energy for ferromagnetic tetragonal martensite can be written as follows:

$$F = \frac{1}{2}C'\varepsilon_{ii}^2 + \frac{1}{2}AM_i^2 - \delta M_i^2\varepsilon_{ii} - M_iH_i \qquad (1),$$

where C' is the elastic modulus, $A \sim \delta(1-c/a)$ is the magnetic anisotropy parameter, δ is a magnetoelastic energy parameter, and H is the magnetic field. Note, that the elastic and magnetoelastic energies in Eq.(1) are expressed for the cubic phase due to negligible 'tetragonal corrections'[24]. The fundamental equation of thermodynamics $\sigma_{ik} = (\partial F/\partial \varepsilon_{ik})_T$ yields:

$$\sigma_{ii} = C'\varepsilon_{ii} + \delta M_i^2 \qquad (2),$$

where a sum of the mechanical stress (first term) and magnetostress (second term) represents a generalized Hooke's law for a stressed ferromagnetic crystal. Eq. (2) shows that the magnetoelastic coupling is responsible for the occurrence of magnetostress. On the other hand, the proportionality between stress and magnetization square confirms a magnetoelastic nature of the field-induced stress. These theoretical findings are supported experimentally [19,22].

In the special case of a linear dependence of the magnetization process as a function of field and $\varepsilon << (1-c/a)$, the magnetoelastic mechanism prescribes the dependence $\varepsilon \sim H^2$ (3) [22-24].

Experimental dependence of the quasielastic reversible MFIS up to 0.5% obtained in Ref. [19] is in agreement with the expression (3).

The field dependence of strain shown in Fig. 2 is only reversible at low fields and relatively small strains, $\varepsilon < 0.5\%$. At larger strains/fields, it is irreversible after field release. The strains corresponding to the plateau in the compression stress-strain curve at zero field shown in the Inset to

Fig. 2 are also irreversible. The results shown in Fig. 2 and Inset were obtained in Refs. [20,21] for a tetragonal 10M-martensitic specimen of Ni51.0Mn27.9Ga21.1 single crystal with T_M=314 K and T_C=370 K. The microstructure of this material, studied in Ref.[21], consists of three martensitic variants, each with an equiprobable volume fraction. Under such conditions, the experimentally obtained maximum strain during specimen compression is about 2%, irrespectively, magnetostress or mechanical force is applied (Fig. 2 and Inset), the last fact being in line with the aforementioned equivalence principle.

The fascinating phenomenon of magnetic-field-induced superelasticity arises when magnetic field and mechanical compression are applied orthogonally to the FSMA specimen, see curve at 2T in the Inset to Fig. 2 [21] and results of Ref. [22]. In this case, alongside a reversible movement of twin boundaries resulting in a recoverable macroscopic deformation of up to 10 % [25,26], a magnetostress value, $\Delta\sigma_M$, can be measured from the difference in a yield stresses, as shown by dash lines in the Inset to Fig. 2. A good agreement between the measured and calculated from a magnetoelastic model values of magnetostress is obtained [22]. So far, the largest value of $\Delta\sigma_M$ (4 MPa) has been shown by the orthorhombic 14M-martensite formed in a $Ni_{51.9}Mn_{26.8}Ga_{21.3}$ single crystal [26].

It is worth noting that according to Eq.(2), a magnetostress depends on the magnetoelastic parameter, magnetization and the mutual orientation of the field and magnetization vector. The parameter δ is seemingly constant in the Ni-Mn-Ga alloy system [19] so, among the material properties, only the saturation magnetization, M_s, can be regulated. Previously, the values of technical saturation magnetization have been measured at room temperature and analyzed as a function of electron concentration [27,28]. Recently, we measured magnetization curves at 77K [29] for all the alloys described in Ref.[6]. The results for the selected alloys with a roughly constant content of the third element are depicted in Fig. 3 and Inset.

Fig. 3 and Inset show different trends in the off-stoichiometry influence on M_s. Substituting Ni or Ga for Mn increases or decreases M_s values, respectively, while at constant concentration of Mn, a substitution of Ni by Ga results in a nonmonotonous behavior of Ms. The maximum of M_s measured at 77 K is found in the vicinity of stoichiometric composition, which is in agreement with results obtained at room temperature [27,28]. Thus, the maximum of magnetostress for the tetragonal 10M-martensite is expected to be achieved in the stoichiometric Ni_2MnGa compound.

STRAIN - INDUCED CHANGE OF MAGNETIZATION EFFECT IN FSMA'S FOR SENSOR APPLICATIONS

In the previous section, results of the uniaxial compression experiments under constant orthogonal magnetic field of 2 T were presented in the Inset to Fig. 2. In the course of the same experiments, it was shown that a nonsaturating field of 0.7 T was also enough to produce a hysteretic reversible stress-strain behavior [21]. The measuring procedure at this field was then modified to register a stray field as a function of compressive strain [21]. The stray filed was measured by a Hall probe on the specimen side facing the applied field. The results are depicted in Fig. 4. Upon deformation, magnetization reduces linearly by up to 30%. Upon unloading, the magnetization restores its initial value with a tiny hysteresis. This effect is reversed with respect to the MFIS one.

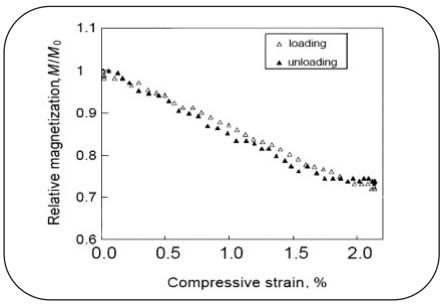

Fig. 4

Magnetization change as a function of strain in the same series of experiments shown in Fig. 2 (see Ref. [21] for details).

Variazione della magnetizzazione in funzione della deformazione applicata nella stesa serie di prove sperimentali mostrata in figura 2 (per dettagli vedere rif. [21]).

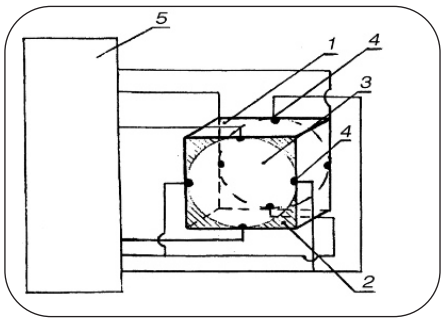

Fig. 5

Sketch of a strain sensor proposed in Ref.[30]: (1) 10M-martensitic parallelepiped of $Ni_{52.0}Mn_{24.4}Ga_{23.6}$ crystal in a single-variant form; (2) insulating layer; (3) permalloy magnetoresistive gauge; (4) electric contacts; (5) amplifier of a differential signal.

Schema di un sensore di deformazione proposto nel rif. [30]: (1) parallelepipedo di martensite-10M di lega $Ni_{52.0}Mn_{24.4}Ga_{23.6}$ in forma di variante singola; (2) strato isolante; (3) estensimetro in permalloy magnetoresistivo; (4) contatti elettrici; (5) amplificatore del segnale differenziale.

A large linear deformation-induced change in magnetization opens new paths towards the implementation of FSMA's in sensors [21,30] and the generation of electric power [31]. A prototype of a strain sensor based on a 10M-martensitic $Ni_{52.0}Mn_{24.4}Ga_{23.6}$ crystal has been suggested in Ref. [30]. A sketch of this sensor design is shown in Fig.6. The parallelepiped-shaped (100)-oriented single-crystal was initially trained (see, e.g., Ref.[5]) in order to obtain a specimen containing only a single-variant of tetragonal martensite. The stress-strain behavior under magnetic field and other characteristics of this specimen are studied in Ref. [22].

For the sensor shown in Fig. 5, a compressive stress to be measured is applied to specimen 1 in a vertical direction. In the initial state, the short c-axis and magnetization vector of the specimen are lying with the horizontal direction in the figure plane. A constant field of about 0.3-0.4 T can be optionally applied in the same horizontal direction to get a reversible operation of the sensor. The magnetic flux change caused by a rotation of the magnetization vector under mechanical staining is registered by a magnetoresistive gauge glued onto an active edge of the specimen. The gauge is made of a permalloy foil with in-plane uniaxial magnetic anisotropy and negligible magnetostriction. The similar foil with its magnetization axis oriented at 90° from the previous one is glued to the opposite edge of specimen. A change in the differential electrical signal of the gauges is calibrated in terms of stress/strain. This signal does not depend on the applied magnetic fields. The sensor has its own noise of less than 10^{-10} V and can be used for both static and dynamic strain/stress measurements.

SUMMARY

In the present paper, some fundamental issues related to the necessary and sufficient conditions of giant MFIS effect in FSMA's were addressed. A Zener type of lattice instability, low restoring force towards (110)[1-10] shear, the thermoelastic martensitic transformation in ferromagnetic matrix and low elastic shear modulus were considered as the necessary conditions for MFIS while both a low yield stress for twin variant rearrangements in martensite, ~1 MPa, and high magnetostress exceeding this yield stress were taken as the sufficient conditions. The most studied prototype Ni-Mn-Ga FSMA system was considered as a

model to illustrate an adequate correspondence between experimental observed phenomena and their theoretical treatment. An application potential of FSMA materials was demonstrated by an implementation in the stress sensor.

ACKNOWLEDGEMENTS

The financial support of the Fondazione Cariplo (project 2004.1819-A10.9251) is gratefully appreciated.

REFERENCES

1) T. KAKESHITA and K.ULLAKKO, MRS Bulletin 2 (2002)p.105.
2) A. N. VASIL'EV, V. D. BUCHEL'NIKOV, T. TAKAGI, V. V. KHOVAILO and E.A. ESTRIN, Physics - Uspekhi 46 (2003) p.559.
3) E. CESARI, J.PONS, R.SANTAMARTA, C.SEGUI and V.A. CHERNENKO, Archives Metal. Mater. 49 (2004) p. 791.
4) S. J. MURRAY, M. MARIONI, S. M. ALLEN, R. C. O'HANDLEY and T. A. LOGRASSO, Appl. Phys. Lett. 77 (2000)p.886.
5) P. MUELLNER, V.A. CHERNENKO and G. KOSTORZ, Mat. Sci.Eng. A 387–389 (2004) p. 965.
6) V.A. CHERNENKO, E.CESARI, V.V.KOKORIN and I.N.VITENKO, Scr.Met.et Mat. 33 (1995)p.1239.
7) F. GEJIMA, Y. SUTOU, R. KAINUMA and K. ISHIDA, Metall. Mater. Trans.A 30 (1999)p.2721.
8) Y. SUTOU, Y. IMANO, N. KOEDA, T. OMORI, R. KAINUMA, K. ISHIDA and K. OIKAWA, Appl. Phys. Lett. 85 (2004) p.4358.
9) K. OIKAWA, L. WULFF, T. IIJIMA, F. GEJIMA, T. OHMORI, A. FUJITA, K.FUKAMICHI, R. KAINUMA and K. ISHIDA, Appl. Phys. Lett. 79 (2001) p.3290.
10) M. WUTTIG, J. LI and C. CRACIUNESCU, Scr. Mater. 44 (2001) p. 2393.
11) K. OIKAWA, T. OTA, Y. SUTOU, T. OHMORI, R. KAINUMA, K. ISHIDA, Mat. Trans. 43 (2002) p.2360.
12) K.OIKAWA, Y. IMANO, V.A. CHERNENKO, F.LUO, T. OMORI, Y. SUTOU, R. KAINUMA, T. KANOMATA and K. ISHIDA, Mat. Trans. 46 (2005) p.734.
13) J. TELLINEN, I. SUORSA, A. JAASKELAINEN, I. AALTIO and K. ULLAKKO, Proc. Actuator 2002 Conference, Bremen, 8 (2002) p. 566.
14) M. KOHL, D. BRUGGER, M. OHTSUKA and T. Takagi, Sensors and Actuators A 114 (2004) p.445.
15) P. G. WEBSTER, K. R. A. ZIEBECK, S. L. TOWN and M. S. PEAK, Phil. Mag. B 49 (1984) p.295.
16) V.A. CHERNENKO, Scr. Mater. 40 (1999) p. 523.
17) V.A. CHERNENKO, J. PONS, C. SEGUI and E. CESARI, Acta Mater. 50 (2002) p. 53.
18) M. STIPCICH, Ll. MANOSA, A. PLANES, M. MORIN, J. ZARETSKY, T. LOGRASSO and C. STASSIS, Phys. Rev.B 70 (2004) 054115.
19) V.A.CHERNENKO, V.A. L'VOV, M.PASQUALE, C.P. SASSO, S.BESSEGHINI and D.A.POLENUR, Int. J. Appl. Electromagn. Mechanics 12 (2000) p.1.
20) P. MUELLNER, V. A. CHERNENKO, M. WOLLGARTEN and G. KOSTORZ, J. Appl. Phys. 92 (2002) p.6708.
21) P. MUELLNER, V. A. CHERNENKO and G. KOSTORZ, Scr. Mater. 49 (2003) p.129.
22) V. A. CHERNENKO, V. A. L'VOV, P. MUELLNER, G. KOSTORZ and T. TAKAGI, Phys. Rev. B69 (2004)134410.
23) V.A. L'VOV, S.P. ZAGORODNYUK and V.A. CHERNENKO, Eur. Phys. J. B 27 (2002) p.55.
24) V.A. CHERNENKO, V.A. L'VOV, S.P. ZAGORODNYUK and T. TAKAGI, Phys. Rev. B 67 (2003) 064407.
25) V. A. CHERNENKO, P. MUELLNER, M. WOLLGARTEN, J. PONS and G. KOSTORZ, J. Phys.IV 112 (2003) p.951.
26) P. MUELLNER, V. A. CHERNENKO and G. KOSTORZ , J. Appl. Phys. 95 (2004) p.1531.
27) X. JIN, M. MARIONI, D. BONO, S. M. ALLEN, R. C. O'HANDLEY and T. Y. HSU, J. Appl.Phys.91 (2002) p.8222.
28) J. ENKOVAARA, O. HECZKO, A. AYUELA and R. M. NIEMINEN, Phys. Rev.B 67 (2003) 212405.
29) V.A. CHERNENKO, S. BESSEGHINI, P. MUELLNER, G.KOSTORZ, J. SCHREUER and M. KRUPA. Sensors Letters V. 5 (2007).p.229.
30) M.M. KRUPA and V.A. CHERNENKO, Patent of Ukraine UA 717551 A. Priority 04-12-2004. Bulletin 12 (2004) p.124.
31) I. SUORSA, J. TELLINEN, K. ULLAKKO and E. PAGOUNIS, J. Appl. Phys. 95 (2004) p.8054.

ABSTRACT

ASPETTI SCIENTIFICI ED APPLICATIVI DEI SISTEMI FERROMAGNETICI A MEMORIA DI FORMA

Parole chiave: leghe a memoria di forma, intermetallici, proprietà, metallurgia fisica

Idealmente, materiali trasduttori dovrebbero esibire ampie deformazioni, generazione di forze elevate e una risposta dinamica pronta. Questi requisiti sono soddisfatti da una nuova classe di materiali denominata leghe a memoria di forma ferromagnetiche (FSMA, Ferromagnetic Shape memory Alloys), che combinano le caratteristiche del ferromagnetismo con quelle di una trasformazione martensitica termoelastica. Finora la maggior parte della ricerca scientifica e tecnologica si è concentrata sulle composizioni del sistema Ni-Mn-Ga che offrono le migliori performance a temperatura ambiente. Per queste leghe è stata sviluppata la tecnologia per la produzione di monocristalli che ha portato alla produzione di attuatori commerciali. Motivato dagli esiti positivi della ricerca sui materiali massivi, vi è anche un grande interesse nello studio di sistemi FSMA in forma di film sottile per applicazioni in microsistemi.

In questa memoria si introducono i principali meccanismi che stanno alla base dell'effetto MFIS (giant magnetic of Mechanical Field Induced Strain) ovvero della deformazione del materiale sotto l'azione di un campo magnetico gigante o di carichi applicati. Viene presentato il modello magnetoelastico, basato sulla teoria di Landau, che consente di sviluppare il concetto di equivalenza tra sforzi meccanici e magnetici. Le principali conseguenze di questo modello sono brevemente discusse.

Si propone anche una rassegna dei più recenti risultati sperimentali, tra cui le anomalie riscontrate nel comportamento stress-strain in campi magnetici di differente intensità, e alcune caratteristiche microstrutturali, ad esempio gli effetti di accoppiamento tra domini magnetici e geminati cristallografici in monocristalli di Ni-Mn-Ga e Co-Ni-Ga. Le opportune considerazioni teoriche permettono di tener conto di questi comportamenti.

In aggiunta sono presentati i risultati più recenti delle ricerche in corso su film sottili magnetici a memoria di forma depositati su differenti substrati, destinati ad applicazioni nel campo dei microattuatori e microsensori. I dati sperimentali sulle trasformazioni ed i domini magnetici osservati sono discussi in termini di microstruttura ed e caratteristiche cristallografiche.